



Synthesis, NMR, X-ray crystallography and DFT studies of some regioisomers possessing imidazole heterocycles

Mustafa Orhan Puskullu^a, Fatima Doganc^b, Seckin Ozden^c, Ertan Sahin^d, Ismail Celik^a, Hakan Goker^{b,*}

^a Department of Pharmaceutical Chemistry, Faculty of Pharmacy, Erciyes University, Kayseri, Turkey

^b Department of Pharmaceutical Chemistry, Faculty of Pharmacy, Ankara University, Ankara, Turkey

^c Department of Pharmaceutical Chemistry, Faculty of Pharmacy, Lokman Hekim University, Ankara, Turkey

^d Department of Chemistry, Faculty of Science, Atatürk University, Erzurum, Turkey



ARTICLE INFO

Article history:

Received 10 May 2021

Revised 27 May 2021

Accepted 28 May 2021

Available online 2 June 2021

Keywords:

Imidazo[4,5-*b*]pyridine

Imidazo[4,5-*d*]pyrimidine

Regioisomer

NOESY

¹H-¹⁵N HMBC

DFT

ABSTRACT

Imidazole-containing heterocycles: Imidazopyridines, imidazopyrimidines can exist in several tautomeric forms. Their regioselectivities were determined for *N*-alkylations with 4-chlorobenzyl bromide under basic conditions (K₂CO₃) in DMF. We observed that, regioisomers were mainly formed as a mixture in this reaction and *N*-benzylation occurs at a higher ratio on six membered heterocycles. Their structural assignments were made with the use of two-dimensional ¹H-¹H NOE (Nuclear Overhauser Effect Spectroscopy, NOESY) and ¹H-¹⁵N HMBC (Heteronuclear Multiple Bond Correlation) spectra. Further confirmation of the structure of **2c** and **3c** were obtained from X-ray crystallography. Experimental data was confirmed by Density Functional Theory (DFT) studies as well.

© 2021 Elsevier B.V. All rights reserved.

1. Introduction

Imidazopyridines and imidazopyrimidines (Purine) are formed by fusing imidazole ring with pyridine and pyrimidine moieties, respectively. These heterocycles have various isomeric forms like imidazo[4,5-*c*]pyridines (**a**), imidazo[4,5-*b*]pyridines (**b**), 9*H*-purine (**c**), 3*H*-purine (**d**) and 1*H*-purine (**e**) (Fig. 1).

Imidazopyridines are attractive heterocycles for medicinal chemists as their derivatives have been shown to exhibit several biological activities. In 2017, a review was reported about pharmacological profiles of imidazopyridines such as anti-tumoral, anti-microbial, anti-inflammatory, anti-diabetic, anti-hypertensive and other pharmacological properties [1]. The NH group present in imidazopyridines is strongly acidic and weakly basic. This group exhibits fast prototropic tautomerism, which leads to equilibrium mixtures. On the other hand, purines play a significant role in living systems. They are basic component of nucleic acids and many commercially used antiviral and antitumor drugs are derivatives of naturally occurring purine bases (adenine and guanine). Various tautomers of purine bases usually coexist due to the presence of several nitrogen sites in the molecule. The preferred tau-

tomers of purine derivatives are mainly *N*⁷-H and *N*⁹-H species, probably due to their lower energy. Existence of this tautomerism, in these bicyclic heterocycles has been shown with spectral data, mainly nuclear magnetic resonance (NMR) spectroscopy. This migration is disappeared when the imidazole hydrogen is replaced by alkyl groups. In our previous studies [2–4], we reported the synthesis of some regioisomers of these cores and their structural assignments were achieved by selective synthesis and/or 2D-NMR techniques. In continuation of these works, here we are addressing the reaction of some 2-(4-fluorophenyl)imidazopyridines and/or 2-(4-fluorophenyl)imidazopyrimidines with 4-chlorobenzyl bromide. Some 2D-NMR techniques including ¹H-¹⁵N HMBC experiment were used for the structural elucidation of regioisomeric products obtained in these reactions. Further confirmation of two compounds were obtained from X-ray crystallography.

2. Results and discussion

Targeted compounds were prepared using the methods outlined in Scheme 1-2. Cyclization of related (*o*-diamino)pyridine and pyrimidine derivatives with sodium metabisulfite adduct of 4-fluorobenzaldehyde gave required imidazo[4,5-*c*]pyridines **1**, imidazo[4,5-*b*]pyridines **2**, imidazo[4,5-*d*]pyrimidines **3**. The regioselective alkylation of one within other nitrogen atoms is dif-

* Corresponding author.

E-mail addresses: goker@ankara.edu.tr, Hakan.Goker@ankara.edu.tr (H. Goker).

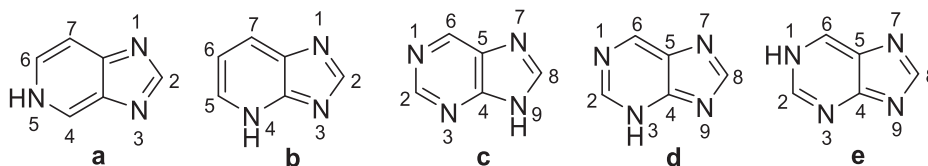
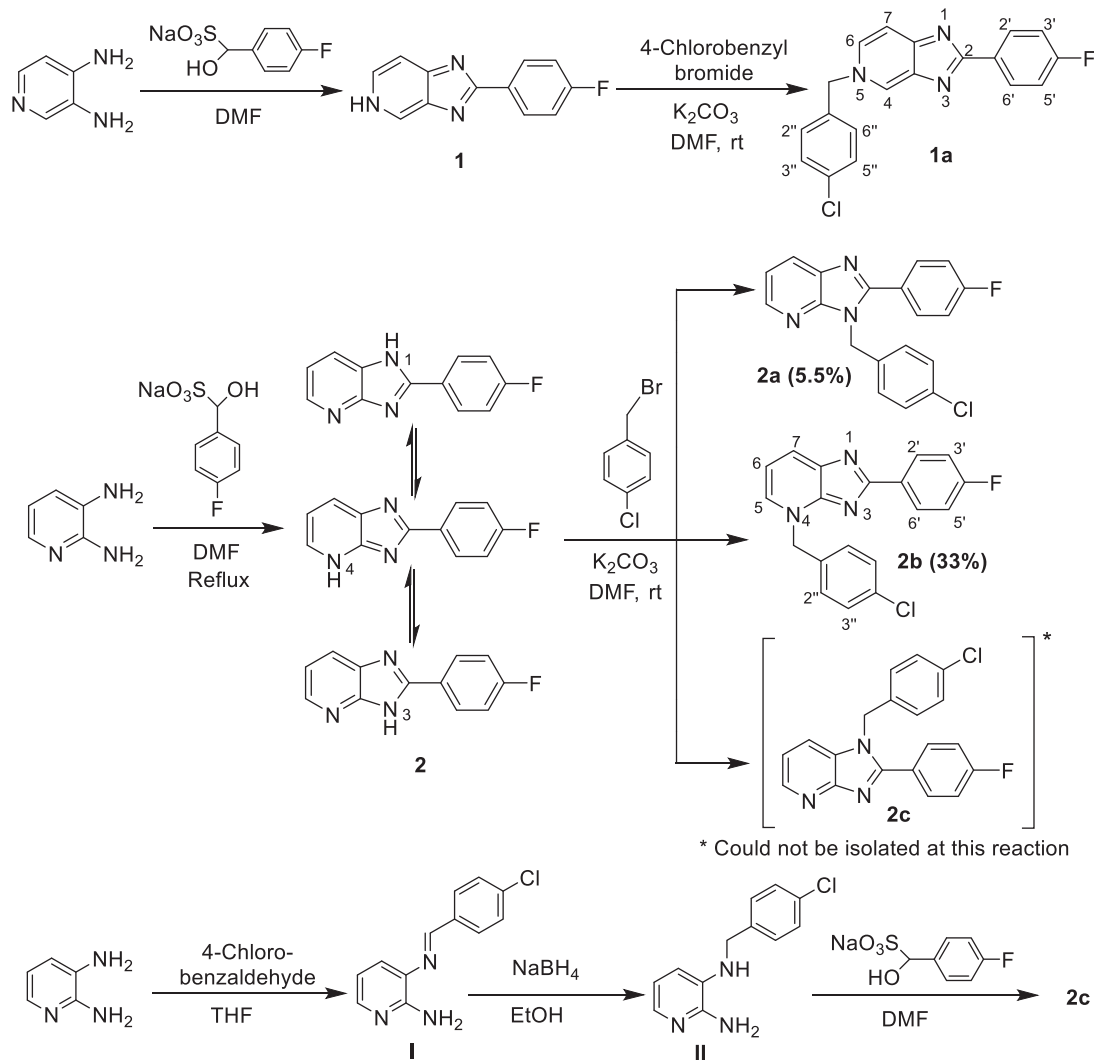


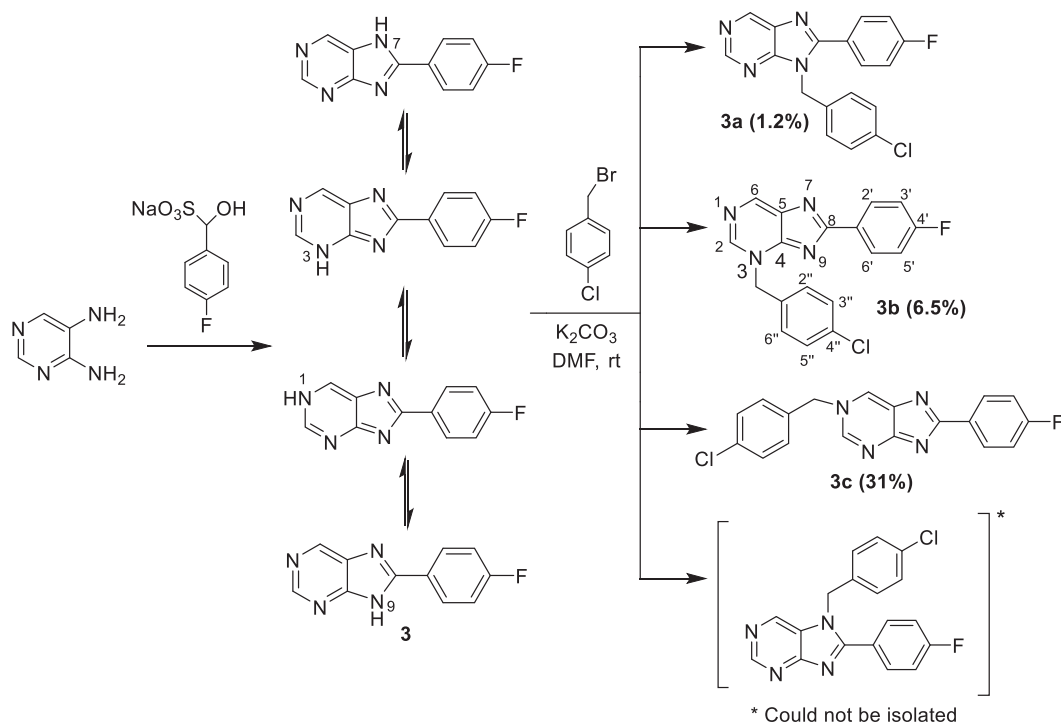
Fig. 1. Some isomeric forms of imidazopyridines and imidazopyrimidines.



Scheme 1. Synthesis of 2-(4-fluorophenyl)imidazopyridine analogues.

difficult, in many cases and giving rise to mixtures of the regioisomers. We reported the *N*-alkylation reaction of some imidazo[4,5-*b*]pyridines in our previous studies [3,4]. It was declared that formation ratio of the regioisomers could be changed with reaction conditions and solvent effects. We aimed to explain some conflict resolutions on the formation of regioisomers. In the literature, there were two different results about the regioisomer formation ratio under same conditions. Short literature review were given on this topic in our previous article [4]. In this study, we have prepared a series of some new 4-fluorophenylimidazo[4,5-*c*]pyridine (**1a**) and 4-fluorophenylimidazo[4,5-*b*]pyridine (**2a-c**) and 4-fluorophenylimidazo[4,5-*d*]pyrimidine (**3a-c**). Targeted compounds **1-3** were prepared by condensation of the corresponding pyrido or pyrimido *o*-diamines with $\text{Na}_2\text{S}_2\text{O}_5$ adduct of 4-fluorobenzaldehydes in DMF (Scheme 1-2). When we attempted alkylation of **1** with 4-chlorobenzyl under basic condi-

tions (K_2CO_3 , DMF), alkylation were formed almost totally only *N*-5 position with high yield (**1a**) as previously reported. Very strong NOE interactions were seen between *N*- CH_2 and H-4,6 in the NOESY spectra of **1a**. These results were also confirmed by HMBC correlations (Fig. 2). In contrast, under same conditions, 4-chlorobenzilation of compound **2** afforded the mixture of regioisomers **2a** (*N*-3) and **2b** (*N*-4) within the yield of 5.5% and 33%, respectively. **2c** (*N*-1) which is the expected 3rd regioisomer were not detected in LC-MS chromatogram. This is why, we have prepared **2c** by selective regioisomer synthesis method, between the reaction **II** and sodium metabisulfite adduct of 4-fluorobenzaldehyde (Scheme-1). Characterisation of the individual isomeric products was determined by observation of 2D-NOESY enhancements between the *N*- CH_2 and H-5,7 protons. In the NOESY spectra of **2a**, there were no NOE contours between benzylic protons and pyridine protons, correlations were seen only be-



Scheme 2. Synthesis of 8-(4-fluorophenyl)purine analogues.

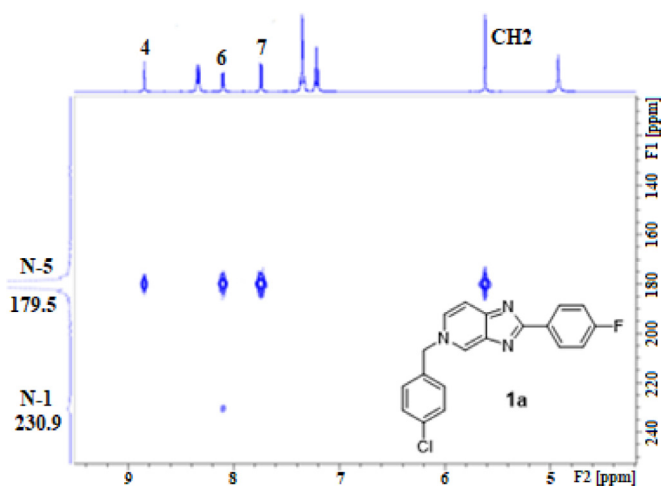


Fig. 2. ^1H - ^{15}N HMBC spectra of compound **1a** (CD_3OD).

tween benzylic and H-2' and/or H-6' as expected. Strong correlations were observed between benzylic and H-5 protons in the spectrum of **2b**. Similarly, cross peaks were observed between $N\text{-CH}_2$ and H-7 proton in the spectrum of **2c**. Complementary structural information was provided by 2D-HMBC spectra of the regioisomers.

It was possible to determine the chemical shift values of C-3a and C-7a, by their correlations with pyridine hydrogens in HMBC spectra. Subsequently, it could be available to determine other possible correlations (whether $N\text{-CH}_2$: C-3a or $N\text{-CH}_2$: C-7a) in separation of regioisomers. The results obtained from the HMBC spectra of **1a**, **2(a-c)** and **3(a-c)** provided all expected correlations. Purine is generally represented when a hydrogen atom is attached to N-9 and it is called $N(9)\text{H}$ tautomer. It is obvious that structures may be considered in which the proton is attached to the other nitrogens of the molecule, yielding the tautomers $N(7)\text{H}$; $N(3)\text{H}$ and $N(1)\text{H}$.

Alkylation of purines usually results with the formation of N -9 and N -7 alkyapurines and frequently N -9 regioisomer is formed as major product. In similar conditions, we achieved the same result with our previous studies and compound **3c** (31%) was obtained as N -1 regioisomer (Scheme-2). In addition, N -3 regioisomer **3b** (6.5%) was also isolated in our conditions; N -3 regioisomers of purines are scarcely reported [4]. In this study, we have isolated N -9 regioisomer as **3a** with 1.2% yield. In NOESY spectrum of **3a**, there was no correlation between the benzylic CH_2 and pyrimidine protons (H-2,6) as expected, interaction was possible with only H-2',6' and H-2'',6''. In contrast, in the NOESY spectra of **3b** and **3c**, while no cross peaks were available between $N\text{-CH}_2$ and H-2',6', but very strong NOE interactions were detected between the $N\text{-CH}_2$ and H-2,6.

On the other hand, in the last quarter, ^1H - ^{15}N heteronuclear multiple-bond correlation (HMBC) experiment was frequently used for measurements of ^{15}N chemical shifts and ^1H - ^{15}N coupling constants [5]. The chemical shifts of ^{15}N nuclei are sensitive indicators for structural analysis of biomacromolecules (nucleic acids, nucleosides, nucleotides, proteins), alkaloids, purine-based antitumor and antiviral drugs and many other organic products. However direct observation of ^{15}N in NMR needs high quantity of sample, because of its low natural abundance (0.37%). At the same time, its NMR sensitivity is very low as well. These difficulties can be partially overcome by using 2D-inverse detected NMR techniques. In particular, ^1H - ^{15}N HMBC experiment has been frequently used for measurements of ^{15}N chemical shifts and ^1H - ^{15}N coupling constants. These parameters are many times employed in structural studies such as tautomerism, protonation, complexation, N -alkylation and N -oxidation processes. Here are the some references report that long-range ^1H - ^{15}N HMBC measurements have been used to differentiate the mixture of some regioisomers [6-11]. We also report here the application of the ^1H - ^{15}N HMBC experiments as a useful tool for regioisomer differentiation. In the ^1H - ^{15}N gHMBC spectrum of **2a** (Fig. 3), long-range coupling of the benzylic hydrogens to the N^3 pyrrole-like nitrogen atom resonance at δ 153 ppm was observed. N^1 pyridine-like nitrogen atom (δ

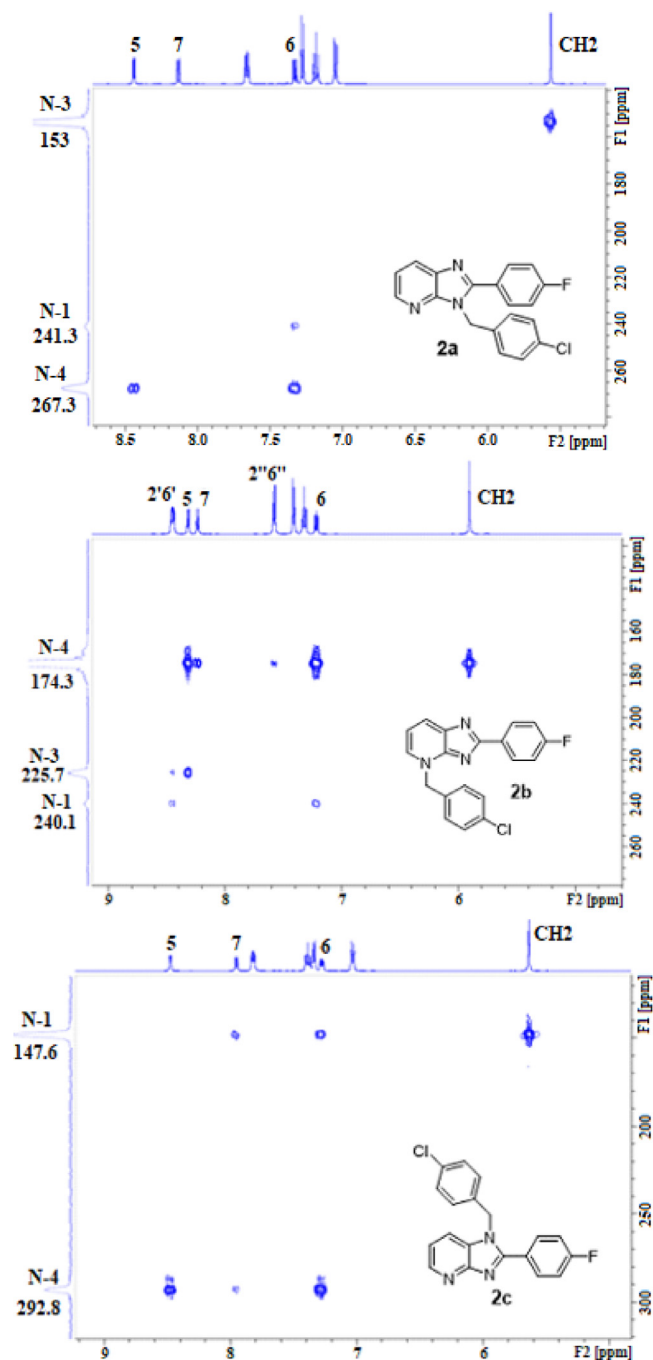


Fig. 3. ^1H - ^{15}N HMBC spectra of compounds **2a** (CDCl_3), **2b** ($\text{DMSO}-d_6$) and **2c** ($\text{DMSO}-d_6$).

241.3 ppm) was correlated with H-6 of the pyridine ring. N^4 pyridine nitrogen atom (δ 267.3 ppm) was strongly correlated with protons H-5,6. Because of the higher π -electron density, pyrrole-like nitrogen atoms are substantially more shielded compared to their pyridine-like counterparts (ca 50–100 ppm), our findings also were in good agreement with the literature data [9,10].

In case of the second regioisomer (**2b**) (Fig. 3), the discriminatory correlations between the benzylic CH_2 protons, H-5,6,7,2',6'' and N^4 nitrogen atom of 1,2-dihydropyridine moiety were observed at δ 174.3 ppm. Correlations were seen from H-5,2',6'' to N^3 at δ 225.7 ppm. The interactions between the H-6,2',6' and N^1 were observed with less intensive contours at 240.1 ppm. For the third regioisomer (**2c**) (Fig. 3), long-range coupling between the benzylic

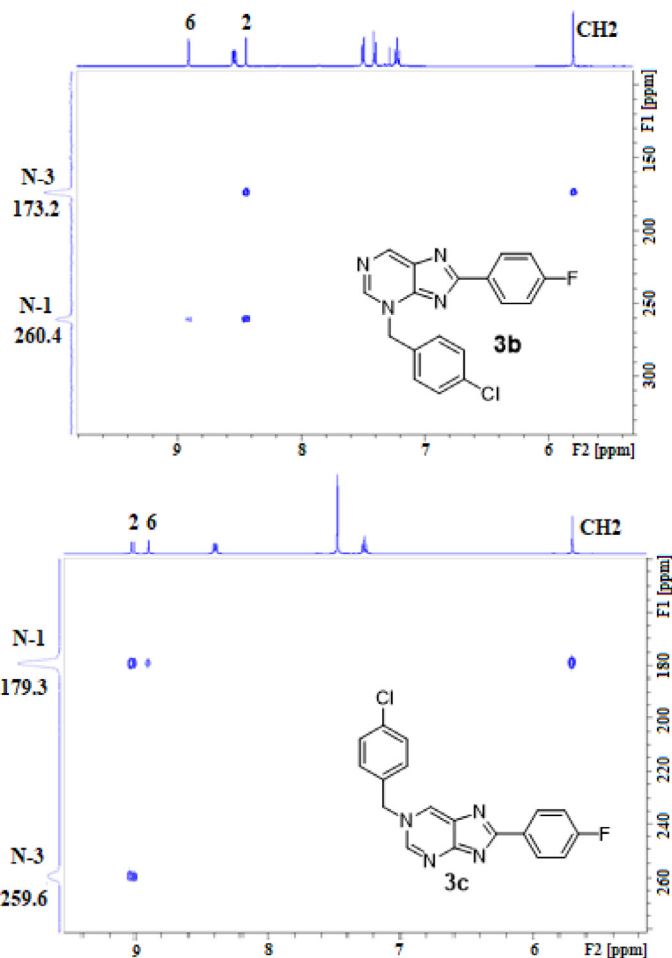


Fig. 4. ^1H - ^{15}N HMBC spectra of compounds **3b** (CDCl_3) and **3c** (CD_3OD).

CH_2 and H-6,7 protons with N^1 pyrrole-like nitrogen atom resonating at δ 147.6 ppm was observed. N^4 pyridine nitrogen atom (292.8 ppm) was coupled with protons H-5,6,7 of the pyridine ring. ^1H - ^{15}N gHMBC experiment is more decisive for the separation of the purine regioisomers. This is the best way to determine which pyrimidine protons are H-2 or H-6.

In the ^1H - ^{15}N gHMBC spectrum of **3b** (Fig. 4), H-2 and benzylic CH_2 protons showed HMBC correlations with N^3 resonating in δ 173.2 ppm. N^1 pyrimidine nitrogen atom δ 260.4 ppm was coupled with protons H-2,6 of the pyrimidine ring. In case of the second regioisomer **3c** (Fig. 4), strong HMBC correlations have been observed between H-2,6, benzylic CH_2 protons and N^1 δ 179.3 ppm. N^3 pyrimidine nitrogen atom δ 259.6 ppm was coupled with protons H-2. All ^1H - ^{15}N HMBC correlations also confirmed the proposed structures of the all regioisomers. Complete analysis of the ^1H and ^{13}C NMR spectra of the synthesized compounds was presented by the aid of 1D and 2D NMR techniques such as COSY, NOESY, gHSQC and gHMBC.

Further confirmation of the structure of **2c** and **3c** were obtained from X-ray crystallography. Their suitable crystals were grown from CHCl_3 solution. The structure of **2c** was solved in the monoclinic space group $\text{P}2_1/c$ with four molecules in the unit cell (Fig. 5). It has imidazopyridine core with substituted 4-fluorophenyl and 4-chlorobenzyl units. Imidazopyridine ring is completely planar. C–C bonds in the pyridine ring are very close to each other (in the range of 1.373–1.399 Å), C–N bond lengths are also approximately equal ($\text{N}1\text{-C}1$ 1.339 Å, $\text{N}1\text{-C}2$ 1.338 Å). These can be attributed to the presence electron delocalization in the

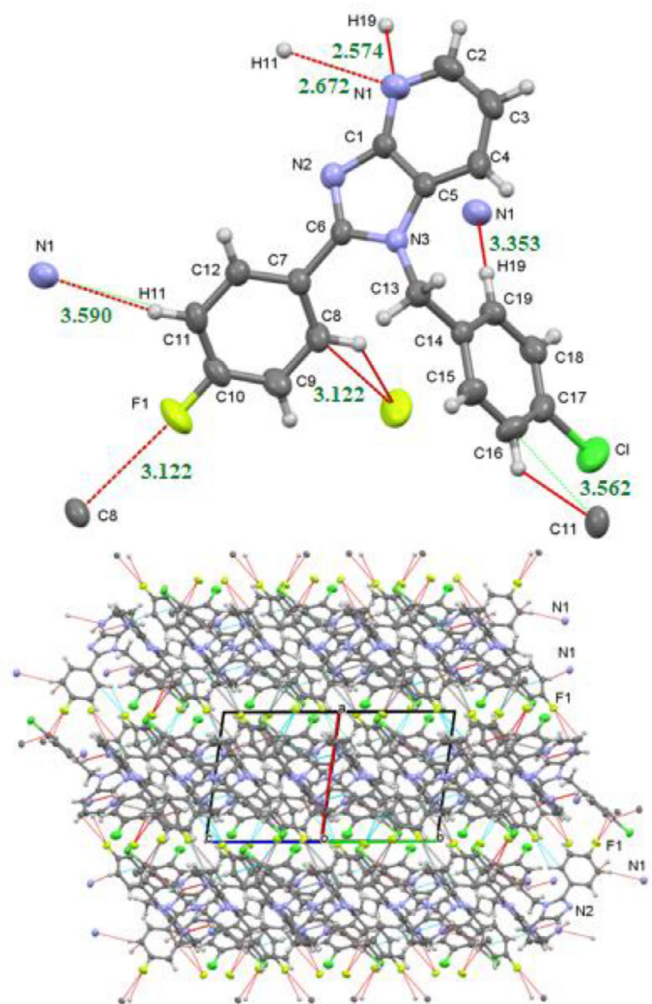


Fig. 5. Up) Molecular structure of **2c** with the short contact geometry less than the sum of vdW radius. Down) Layered stacking and short contact geometry of the molecule **2c** viewed down along the diagonal [011] axis.

pyridine ring. In the imidazol unit, the single and double bonds are more clearly separated than each other (N2-C6 1.316 Å, N2-C1 1.378 Å). The dihedral angle between the C7/C12 and the C14/C19 aromatic plane is 58.7°. Dihedral angles between these rings and imidazopyridine plane are 45.4° and 74.2°, respectively. Deviation from planarity of the molecule is due to significant steric effects and intermolecular interactions. The crystal structure is also stabilized by the intramolecular C8-H8...F1 [$D\cdots A = 3.122(3)$ Å] and C19-H19...N1 [$D\cdots A = 3.353(3)$ Å] interactions. The π - π stacking interactions between the delocalized π -electrons of the phenyl rings are weak. The distance between the rings centroids are in the range of 3.96–5.64 Å.

Structure of **3c** was also solved in the monoclinic space group P2₁/c (Fig. 6). It has imidazopyrimidine core with substituted 4-fluorophenyl and 4-chlorobenzyl units. Purine ring is almost in the same plane as the 4-fluorophenyl group. The dihedral angle between the chlorophenyl and purine mean planes is 85.2°. Here, purine heterocycle has 1*H*-purine (**e**) isomeric forms (Fig. 1). C=N double bonds in the ring are as follows; N4=C11 1.328(3) Å, N3=C12 1.335(3) Å and N2=C8 1.302 Å. Meanwhile, intermolecular C7-H...N1 [$D\cdots A = 3.437(3)$ Å], C9-H...N4 [$D\cdots A = 3.493(3)$ Å] and C-H... π (4.0 Å) interactions have a contribution in the formation of a stable structure. The π - π stacking distances are in the range of 3.53–5.97 Å.

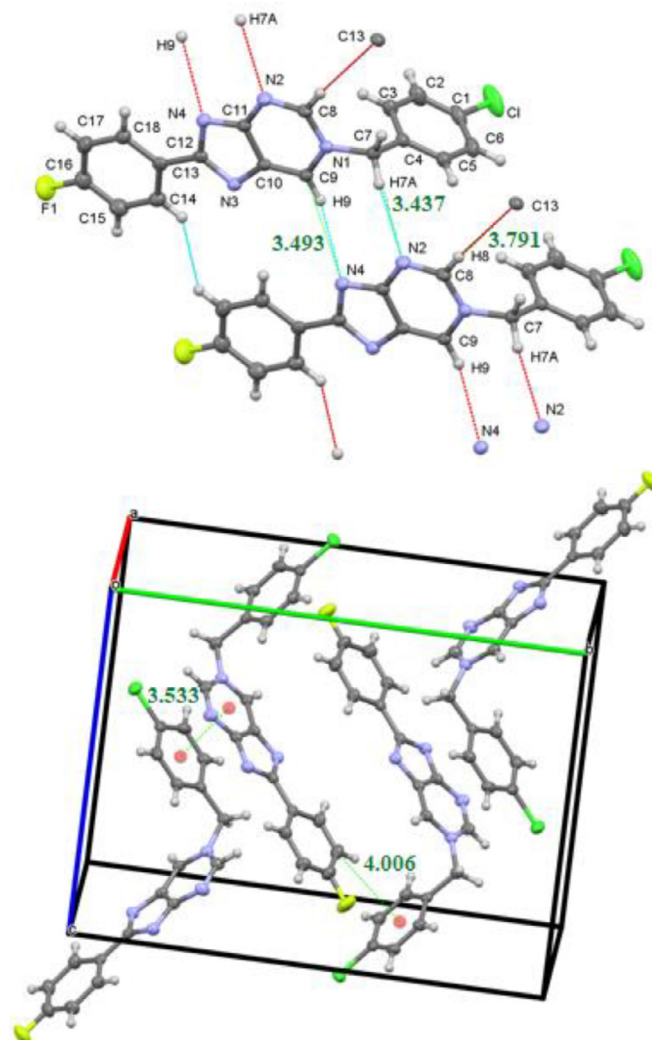


Fig. 6. Up) Molecular structure of **3c** with the short contact geometry (less than the sum of vdW radius). Down) C-H... π and π - π stacking interactions of the molecule **3c** with the unit cell viewed down along the *a*-axis.

3. Geometric optimization, frontier molecular orbital, and molecular electrostatic potentials analysis

In terms of computational studies, it is important to estimate the 3D structure of a compound and to calculate the bond length and angle in atoms. Prediction of the lowest energy structure of the compound is mainly used in organic and medicinal chemistry in many areas such as molecular docking, molecular dynamics simulations, quantitative structure-activity relationship, and theoretical ADME calculations [12,13]. Accordingly, the optimized geometric structures of the synthesized resulting products were determined and shown in Figs. 7 and 8. Frontier molecular orbital analysis of the compounds was performed. Gap ΔE : ($E_{\text{LUMO}} - E_{\text{HOMO}}$), IP (-HOMO): ionization potential, EA (-LUMO): electron affinity, X ($(IP+EA)/2$): electronegativity, η ($(IP-EA)/2$): chemical hardness, S ($1/2\eta$): chemical softness, μ $-(IP+EA)/2$: chemical potential, ω ($\mu^2/2\eta$): electrophilic index values were calculated. The HOMO value is a measure of the electron-donating capacity of the molecule, that is a parameter indicating the nucleophilicity of the molecule. LUMO, on the other hand, is a measure of the electron withdrawal capacity, which expresses the electrophilicity of the molecule. As shown in Figs. 7 and 8, the HOMO and LUMO orbitals of all the compounds were localized on the imidazopy-

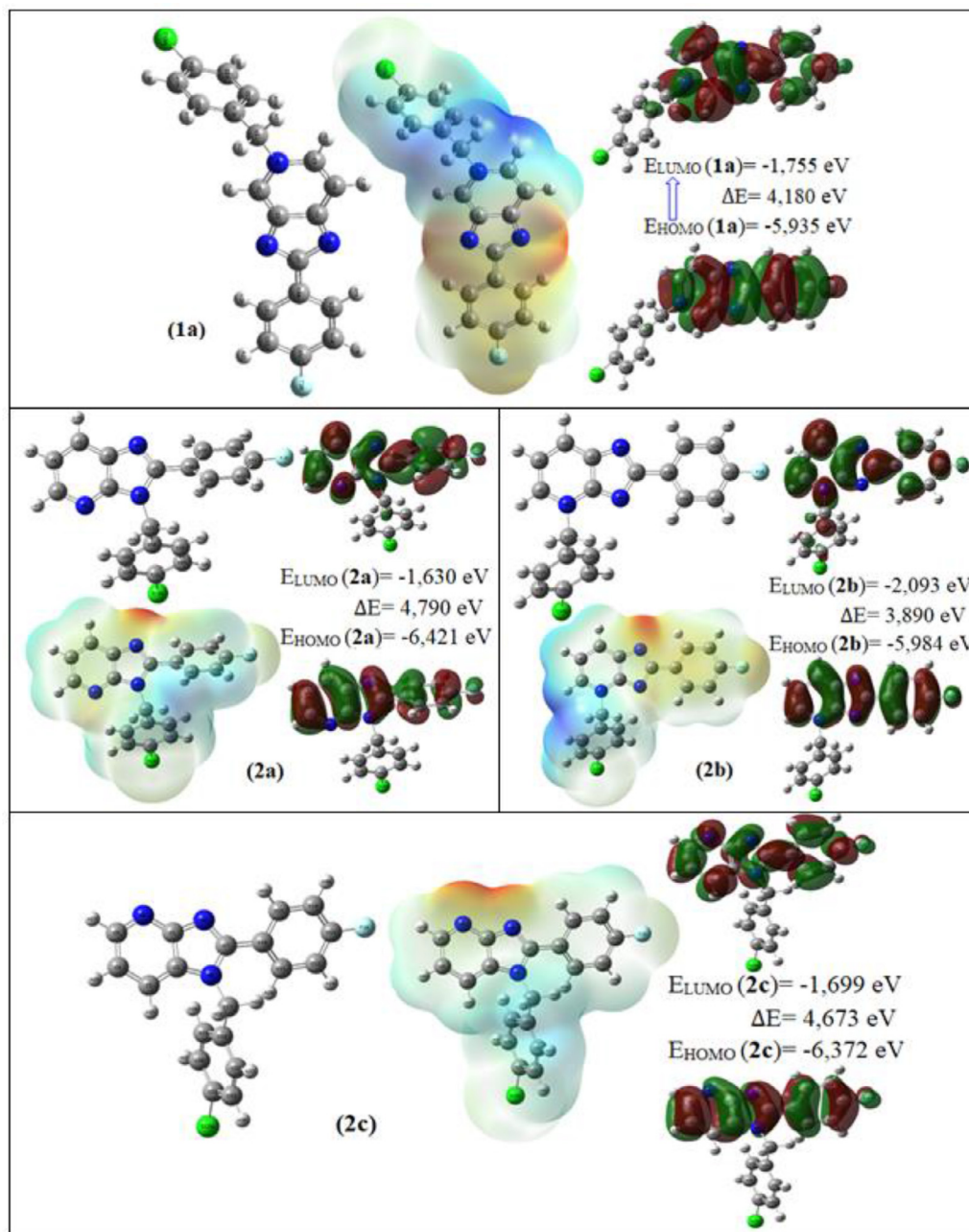


Fig. 7. Optimized structures (left), molecular electrostatic potential (MEP) of highest-occupied molecular orbital (HOMO) - lowest-unoccupied molecular orbital (LUMO) diagram (right) of the compounds **1a**, **2a**, **2b** and **2c**.

ridine/pyrimidine ring and the phenyl ring at the 2nd position. HOMO orbitals C1-C2-C6 of the benzene atom in 2nd position and C3-C4-C5 are localized on ternary atoms at their positions. They are localized on the first three atoms of the imidazo structure and three atoms of the pyridine/pyrimidine structures adjacent to them and two adjacent carbon atoms. LUMO is localized on the C2-C3 and C5-C6 atoms of the benzene ring attached to the imidazo ring at the 2nd position. Specific LUMO orbitals are localized on the carbon at the 2nd position of the imidazo ring and the carbon of the benzene ring attached to it. LUMO orbitals were formed on the first carbon atom of the substituted benzene atom from nitrogen atoms attached to the imidazo, pyridine or pyrimidine ring.

The gap value is also a value that numerically gives the electron transition state of the molecule in HOMO to LUMO and this value is a measure of the chemical stability of the compound. Ionization

energy, also called ionization potential, is the amount of energy required to remove an electron from an isolated atom or molecule. Electron affinity reflects an atom's ability to accept an electron. It shows the energy change that occurs when an electron is added to a gaseous atom. Electronegativity, which expresses numerically the tendency of an atom to attract electrons in a molecule, is a semi-qualitative quantity. Chemical hardness is a measure of the stability of the molecule and substances with high chemical hardness do not polarize easily and react more difficultly. Chemical softness is an approach that expresses the molecule is easier to polarize and react to. The chemical potential reflects the ease with which an electron is delivered from the system in its ground state. The electrophilic index is another measure of the electron-donating capacity [14,15].

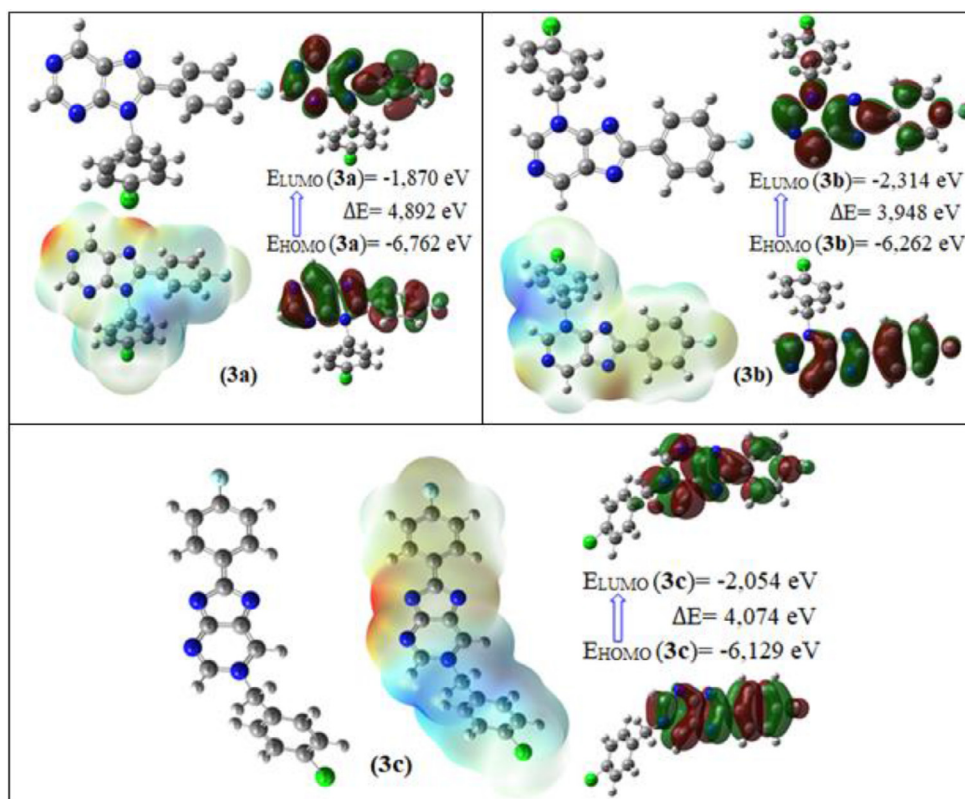


Fig. 8. Optimized structures (left), molecular electrostatic potential (MEP) of highest-occupied molecular orbital (HOMO) - lowest-unoccupied molecular orbital (LUMO) diagram (right) of the compounds **3a**, **3b** and **3c**.

Table 1

Quantum parameters of imidazole-containing heterocycles compound **1a**, **2a**, **2b**, **2c**, **3a**, **3b** and **3c**.

Comp.	LUMO	HOMO	Gap ΔE	IP	EA	X	η	S	μ	ω
1a	-1,755	-5,935	4,180	5,935	1,755	3,845	2,090	0,239	-3,845	3,538
2a	-1,630	-6,421	4,790	6,421	1,630	4,026	2,395	0,209	-4,026	3,383
2b	-2,093	-5,984	3,890	5,984	2,093	4,039	1,945	0,257	-4,039	4,192
2c	-1,699	-6,372	4,673	6,372	1,699	4,036	2,337	0,214	-4,036	3,485
3a	-1,870	-6,762	4,892	6,762	1,870	4,316	2,446	0,204	-4,316	3,808
3b	-2,314	-6,262	3,948	6,262	2,314	4,288	1,974	0,253	-4,288	4,657
3c	-2,054	-6,129	4,074	6,129	2,054	4,092	2,037	0,245	-4,092	4,109

Gap ΔE : ($E_{LUMO} - E_{HOMO}$), IP (**-HOMO**): Ionization potential, EA (**-LUMO**): Electron affinity, X ($(IP+EA)/2$): Electronegativity, η ($(IP-EA)/2$): Chemical hardness, S ($1/2\eta$): chemical softness, μ ($-(IP+EA)/2$): Chemical potential, ω ($\mu^2/2\eta$): Electrophilic index.

As given in **Table 1**, **3b** has the highest LUMO energy, electron affinity, chemical softness and electrophilic index amongst all compounds. On the other hand, compound **3a** has the highest HOMO energy, gap, ionization potential, electronegativity, chemical hardness and chemical potential. The fact that the chlorobenzyl group is in the 3rd and 9th positions carries the quantum parameters of the compound to the highest and lowest levels.

The MEP plot is used to qualitatively understand the 3D electronic properties and charges of a compound through colors. In this plot, the red areas are the regions of high electron density, the blue areas are low electron density regions, yellow areas less electron and green indicates neutral regions [16]. As shown in **Figs. 7** and **8**, the electron density around the nitrogen atoms of the imidazole ring is high. The status of the red regions varies depending on the substitution of imidazole, pyridine, or pyrimidine nitrogens. The benzene in the 2nd position and the variable benzyl group are the neutral regions. The electron density of the aliphatic hydrogens of the benzyl group is the least.

4. Conclusions

It was found that *N*-benzylation of imidazo[4,5-*c*]pyridine, imidazo[4,5-*b*]pyridine and imidazo[4,5-*d*]pyrimidine (Purine) favourably was realized on the six membered *N*-heterocycles in presence of anhydrous K_2CO_3 in DMF. Because of the very similar polarities of imidazole *N*-alkylated products, they cannot be easily separated from each other's by column chromatography. However, it is possible to separate *N*-alkylated six membered regioisomers from the imidazole *N*-alkylated regioisomers. In our experiments, imidazole *N*-alkylated regioisomers were obtained firstly from the column chromatography. NOESY experiment is the primary method for structural elucidation of these types of regioisomers. The cross peaks of *N*-CH₂ (at around 5–6 δ ppm) and aromatic protons confirm their spatial proximity as an evidence for which nitrogen atom is substituted. 1H - ^{13}C and 1H - ^{15}N HMBC techniques can be an effective alternative method for assignment of regioisomers. The complete structure elucidation of all synthesized

compounds was performed using 1D and 2D NMR experiments including COSY, NOESY, gHSQC, gHMBC and XRD data.

5. Material and method

5.1. Chemistry

Uncorrected melting points were measured on an Büchi B-540 capillary melting point apparatus. ^1H (400 and 500 MHz) and ^{13}C (100 and 125 MHz) NMR spectra were recorded employing a Varian Mercury (AGILENT) 400 MHz and BRUKER AVANCE NEO 500 MHz FT spectrometers, chemical shifts (δ) are in ppm relative to TMS. The samples (5–15 mg) were prepared in 0.75 ml of DMSO- d_6 , CDCl_3 and CD_3OD . TMS was used as an internal standard. The liquid chromatography mass spectrometry (LC-MS) spectra were taken on a Waters Micromass ZQ connected with Waters Alliance HPLC (Waters Corporation, Milford, MA, USA), using the ESI(+) method with a C-18 column (XTerra®, 4.6×250 mm, $5 \mu\text{m}$).

5.1.1. Synthesis of sodium metabisulfite adduct of 4-fluorobenzaldehyde

4-Fluorobenzaldehyde (7.5 mmol) was dissolved in EtOH (25 mL) and sodium metabisulfite (0.8 g) (in 5 mL of water) was added in portions. The reaction mixture was stirred vigorously and more EtOH was added. The mixture was kept in a refrigerator for a while. The white precipitate, the obtained salts were gained by filtration, dried and used for the further steps without purification and characterization.

5.1.2. General synthesis of 1, 2, 3

The mixture of sodium metabisulfite adduct of 4-fluorobenzaldehyde (1 mmol) and corresponding 2,3-diamine pyridine or 4,5-diaminopyrimidine (1 mmol), in DMF (2 mL) were heated at 120°C , for 3–4 h. The reaction mixture was cooled, poured into water. The resulting precipitate was collected by filtration and boiled in EtOH filtered and dried.

5.1.2.1. 2-(4-Fluorophenyl)-5H-imidazo[4,5-c]pyridine (1). Prepared from 3,4-diaminopyridine (0.11 g) as described in general method. Yield 0.16 g, 75%, mp > 275°C . $^1\text{H NMR}$ δ ppm (DMSO- d_6): 7.43–7.48 (m, 2H, H-3',5'), 7.69 (d, 1H, $J = 5.6$ Hz, H-7), 8.29–8.33 (m, 2H, H-2',6'), 8.36 (d, 1H, $J = 5.6$ Hz, H-6), 9.03 (s, 1H, H-4); $^{13}\text{C NMR}$ (DMSO- d_6): 163.6 (d, $J = 247$ Hz, C-4'), 153.7, 143.4, 139.9, 138.5, 137.8, 129.5 (d, $J = 9$ Hz, C-2',6'), 125.85 (d, $J = 3.2$ Hz, C-1'), 116.2 (d, $J = 22$ Hz, C-3',5'), 109.3; **MS** (ESI+) m/z : 214 ($M + H$, 100%), $\text{C}_{12}\text{H}_8\text{FN}_3$. (HCl salt available in lit.^[17]).

5.1.2.2. 2-(4-Fluorophenyl)-3H-imidazo[4,5-b]pyridine (2). Prepared from 2,3-diaminopyridine (0.11 g) as described in general method. Yield 0.195 g, 91%, mp: $288\text{--}290^\circ\text{C}$, lit.^[18] $289\text{--}290^\circ\text{C}$. $^1\text{H NMR}$ δ ppm (DMSO- d_6): 7.25 (dd, 1H, $J = 7.6$ & 4.8 Hz, H-6), 7.4–7.45 (m, 2H, H-3',5'), 8.02 (br.d, 1H, $J = 6.8$ Hz, H-7), 8.29–8.32 (m, 2H, H-2',6'), 8.36 (br.d, 1H, $J = 3.6$ Hz, H-5), 13.5 (br.s, NH); $^{13}\text{C NMR}$ (DMSO- d_6): 163.4 (d, $J = 247$ Hz, C-4'), 151.7, 143.7, 129.0 (d, $J = 8.9$ Hz, C-2',6'), 126.22 (d, $J = 3$ Hz, C-1'), 117.95, 115.9 (d, $J = 22$ Hz, C-3',5'); **MS** (ESI+) m/z : 214 ($M + H$, 100%), $\text{C}_{12}\text{H}_8\text{FN}_3$. (NMR data are consistent with lit.^[19]).

5.1.2.3. 8-(4-Fluorophenyl)-9H-purine (3). Prepared from 4,5-diaminopyrimidine (0.11 g) as described in general method. Yield 0.155 g, 72%, mp: $325\text{--}326^\circ\text{C}$. $^1\text{H NMR}$ δ ppm (DMSO- d_6): 7.41–7.45 (m, 2H, H-3',5'), 8.27–8.31 (m, 2H, H-2',6'), 8.87 (s, 1H, H-6), 9.1 (s, 1H, H-2); $^{13}\text{C NMR}$ (DMSO- d_6): 163.8 (d, $J = 249$ Hz, C-4'), 152.0, 129.7 (d, $J = 8.9$ Hz, C-2',6'), 125.5, 116.2 (d, $J = 22$ Hz, C-3',5'); **MS** (ESI+) m/z : 215 ($M + H$, 100%), $\text{C}_{11}\text{H}_7\text{FN}_4$.

5.1.3. 3-[(4-Chlorobenzylidene)amino]pyridine-2-amine (I)

To a suspension of 2,3-diaminopyridine (0.36 g, 3.3 mmol) in THF (33 mL), dried molecular sieves (2 g, 4 Å) and 4-chlorobenzaldehyde (0.55 g, 3.9 mmol) were added. After refluxing for 4 h, the mixture was stirred overnight. The reaction mixture was filtered and concentrated, the residue was purified by silica gel column chromatography and eluted with *n*-Hexane: EtOAc (70:30) to (30–70) gradient, mp: $141\text{--}143^\circ\text{C}$, lit.^[20] 143°C , yield 0.55 g, 72.4%. $^1\text{H NMR}$ (CDCl_3) δ ppm: 5.3 (br.s, 2H, N \underline{H}_2), 6.59 (dd, 1H, $J = 5.6$ & 5.2 Hz, H-5), 7.17 (d, 1H, $J = 8$ Hz, H-4), 7.37 (d, 2H, $J = 8$ Hz, H-3',5'), 7.76 (d, 2H, H-2',6'), 7.95 (d, 1H, $J = 8$ Hz, H-6), 8.38 (s, 1H, N=CH); $^{13}\text{C NMR}$ (CDCl_3) δ ppm: 157.5, 154.9, 146.6, 137.4, 134.5, 131.6, 129.9, 129.1, 123.3, 113.8; **MS** (ESI+) m/z : 232 ($M + H$, 100%), 234 ($M + H$, 34%), $\text{C}_{12}\text{H}_{10}\text{ClN}_3$.

5.1.4. N^3 -(4-Chlorobenzyl)pyridine-2,3-diamine (II)

Compound **I** (0.5 g, 2.15 mmol) was dissolved in ethanol (30 mL) and treated with sodium borohydride (0.6 g, 15.86 mmol). After refluxing for 8 h, water was added and a light yellow coloured powder was filtered, dried and crystallised from used EtOAc: *n*-Hexane; yield 0.45 g, 90%, mp: $136\text{--}138^\circ\text{C}$. $^1\text{H NMR}$ (CDCl_3) δ ppm: 3.62 (br.t, 1H, N $\underline{H}\text{-CH}_2$), 4.22–4.27 (m, 4H, NH-C \underline{H}_2 & 2-N \underline{H}_2), 6.65 (dd, 1H, $J = 7.6$ & 5.2 Hz, H-5), 6.74 (dd, 1H, $J = 7.6$ & 1.2 Hz, H-4), 7.28–7.33 (m, 4H, H-2',6',3',5'), 7.61 (dd, 1H, $J = 5.2$ & 1.6 Hz, H-6); $^{13}\text{C NMR}$ (CDCl_3) δ ppm: 148.8, 137.2, 137.0, 133.2, 131.5, 128.88, 128.83, 117.6, 115.85, 47.5; **MS** (ESI+) m/z : 234 ($M + H$, 100%), 236 ($M + H$, 34%), $\text{C}_{12}\text{H}_{12}\text{ClN}_3$.

5.1.5. General synthesis of 1a, 2a-b, 3a-c

K_2CO_3 (0.138 g, 1 mmol) was added to a suspension of the **1–3** (0.7 mmol) in DMF (0.5 mL) and stirred. One hour later, 4-chlorobenzyl bromide (0.12 g, 0.75 mmol) was added. After overnight stirring at room temperature, water was added and precipitate was filtered.

5.1.5.1. 5-(4-Chlorobenzyl)-2-(4-fluorophenyl)-5H-imidazo[4,5-c]pyridine (1a). Prepared from **1** (0.15 g) as described in general method. Crude product was purified column chromatography by using CH_2Cl_2 : MeOH (95: 5), white solid, yield 0.130 g, 55%, mp: $229\text{--}232^\circ\text{C}$. $^1\text{H NMR}$ δ ppm (CD_3OD): 5.65 (s, 2H, benzylic C \underline{H}_2), 7.2–7.26 (m, 2H, H-3',5'), 7.36–7.41 (m, 4H, H-2',6'',3'',5''), 7.76 (d, 1H, $J = 6.8$ Hz, H-7), 8.13 (dd, 1H, $J = 6.8$ & 1.6 Hz, H-6), 8.32–8.36 (m, 2H, H-2',6'), 8.87 (d, 1H, $J = 1.6$ Hz, H-4); **COSY**: [H-6: H-7], [H-6: H-4 (secondary)], [H-2',6': H-3',5']; **NOESY**: [Benzylic C \underline{H}_2 : H-4 / H-6 / H-2',6'']; $^{13}\text{C NMR}$, **HSQC** & **HMBC** (CD_3OD): 171.85 (C-2), 165.6 (d, $J = 247.5$ Hz, C-4'), 156.8 (C-7a), 146.0 (C-3a), 136.1 (C-4''), 135.6 (C-1''), 133.5 (C-6H), 132.7 (C-4H), 131.4 (d, $J = 8.4$ Hz, C-2',6'H), 131.33 (d, $J = 3$ Hz, C-1'), 130.8 (C-2'',6''H), 130.5(C-3'',5''H), 116.6 (d, $J = 22$ Hz, C-3',5'H), 113.75 (C-7H), 62.9 (Benzylic $\underline{C}\text{H}_2$); $^1\text{H-}^{15}\text{N HMBC}$ (CD_3OD): [N^5 (179.5 δ ppm) / H-4,6,7 & benzylic CH_2], [N^1 (230.9 δ ppm) / H-6]; **MS** (ESI+) m/z : 338 ($M + H$, 100%), 340 ($M + H + 2$, 32%), 124 ($M + H$, 85%), 126 ($M + H + 2$, 28%), $\text{C}_{19}\text{H}_{13}\text{ClFN}_3$.

5.1.5.2. 3-(4-Chlorobenzyl)-2-(4-fluorophenyl)-3H-imidazo[4,5-b]pyridine (2a) and 4-(4-Chlorobenzyl)-2-(4-fluorophenyl)-4H-imidazo[4,5-b]pyridine (2b). Prepared from **2** (0.15 g) as described in general method. Purification [CH_2Cl_2 : MeOH (100: 4)] of the crude powder first afforded **2a** as white a solid, yield 0.013 g, 5.5%, mp: $157\text{--}160^\circ\text{C}$. $^1\text{H NMR}$ (CDCl_3) δ ppm: 5.54 (s, 2H, benzylic C \underline{H}_2), 7.02 (d, 2H, $J = 8$ Hz, H-2',6''), 7.14–7.18 (m, 2H, H-3',5'), 7.24 (d, 2H, $J = 8$ Hz, H-3',5''), 7.3 (dd, 1H, $J = 4.8$ & 8 Hz, H-6), 7.62–7.66 (m, 2H, H-2',6'), 8.1 (dd, 1H, $J = 6.8$ & 1.2 Hz, H-7), 8.41 (dd, 1H, $J = 8$ & 1.2 Hz, H-5); **COSY**: [H-6: H-5], [H-6: H-7], [H-2',6': H-3',5'], [H-2',6'': H-3',5'']; **NOESY**: [Benzylic C \underline{H}_2 : H-2',6' / H-2',6'']; $^{13}\text{C NMR}$, **HSQC** & **HMBC** (CDCl_3) δ ppm: 164

(d, $J = 251$ Hz, C-4'), 153.7 (C-2), 148.7 (C-3a), 144.5 (C-5H), 135.1 (C-1''), 134.8 (C-7a), 133.75 (C-4''), 131.2 (d, $J = 8$ Hz, C-2',6'H), 129.1 (C-3'',5''H), 127.9 (C-2'',6''H), 127.4 (C-7H), 125.8 (d, $J = 3$ Hz, C-1'), 119.15 (C-6H), 116.1 (d, $J = 22$ Hz, C-3',5'H), 46.2 (benzylic carbon); **¹H-¹⁵N HMBC** (CDCl₃): [N^3 (153 δ ppm): benzylic CH₂], [N^1 (241.3 δ ppm): H-6], [N^4 (267.3 δ ppm): H-5 / H-6]; **MS** (ESI+) m/z : 338 ($M + H$, 100%), 340 ($M + H + 2$, 32%), 124 ($M + H$, 100%), 126 ($M + H + 2$, 32%), C₁₉H₁₃ClFN₃.

Continued elution CH₂Cl₂: MeOH (100: 4) provided **2b** as a white solid, yield 0.09 g, 33%, mp: 128–130°C. **¹H NMR** (DMSO-*d*₆) δ ppm: 5.90 (s, 2H, benzylic C H₂), 7.22 (dd, 1H, $J = 7.2$ & 6 Hz, H-6), 7.29–7.34 (m, 2H, H-3',5'), 7.42 (d, 2H, $J = 8.4$ Hz, H-3'',5''), 7.57 (d, 2H, $J = 8.4$ Hz, H-2'',6''), 8.23 (d, 1H, $J = 8$ Hz, H-7), 8.31 (d, 1H, $J = 5.6$ Hz, H-5), 8.4–8.44 (m, 2H, H-2',6'); **COSY**: [H-6: H-5], [H-6: H-7], [H-2',6': H-3',5'], [H-2'',6'': H-3'',5'']; **NOESY**: [Benzylic C H₂: H-5 / H-2'',6'']; **¹³C NMR, HSQC & HMBC** (DMSO-*d*₆) δ ppm: 166.9 (C-2), 163.2 (d, $J = 245$ Hz, C-4'), 153.6 (C-3a), 145.0 (C-7a), 134.7 (C-1''), 133.1 (C-4''), 131.2 (C-5H), 131.1 (d, $J = 2.6$ Hz, C-1'), 130.3 (C-2'',6''H), 129.7 (d, $J = 9$ Hz, C-2',6'H), 128.7 (C-3'',5''H), 127.9 (C-7H), 115.5 (d, $J = 21$ Hz, C-3',5'H), 113.2 (C-6H), 55.1 (benzylic carbon); **¹H-¹⁵N HMBC** (DMSO-*d*₆): [N^4 (174.3 δ ppm): H-7 / H-6 / H-5 / H-2'',6'' / benzylic C H₂], [N^3 (225.7 δ ppm): H-5 / H-2',6'], [N^1 (240.1 δ ppm): H-6 / H-2',6']; **MS** (ESI+) m/z : 338 ($M + H$, 100%), 340 ($M + H + 2$, 32%), 124 ($M + H$, 85%), 126 ($M + H + 2$, 28%), C₁₉H₁₃ClFN₃.

5.1.5.3. 1-(4-Chlorobenzyl)-2-(4-fluorophenyl)-1H-imidazo[4,5-b]pyridine (2c). A mixture of **II** (0.233 g, 1 mmol) and Na₂S₂O₅ adduct of 4-fluorobenzaldehyde (0.228 g, 1 mmol) in DMF (0.4 mL) was heated at 120°C for 4 h. Water was added, the resulting precipitate was filtered and dried. Precipitate was crystallised from CHCl₃: *n*-Hexane as colourless crystals, yield 0.25 g, 73.7%, mp: 202–204°C. **¹H NMR** (DMSO-*d*₆) δ ppm: 5.63 (s, 2H, benzylic C H₂), 7.02 (d, 2H, $J = 8.4$ Hz, H-2'',6''), 7.27 (dd, 1H, $J = 7.8$ & 4 Hz, H-6), 7.34 (d, 2H, $J = 8.4$ Hz, H-3'',5''), 7.37–7.40 (m, 2H, H-3',5'), 7.80–7.83 (m, 2H, H-2',6'), 7.94 (dd, 1H, $J = 8$ & 1.2 Hz, H-7), 8.46 (dd, 1H, $J = 4.8$ & 1.2 Hz, H-5); **COSY**: [H-6: H-5], [H-6: H-7], [H-2',6': H-3',5'], [H-2'',6'': H-3'',5'']; **NOESY**: [N^1 -C H₂: H-7 / H-2',6' / H-2'',6'']; **¹³C NMR, HSQC & HMBC** (DMSO-*d*₆) δ ppm: 163.1 (d, $J = 248$ Hz, C-4'), 155.0 (C-3a), 154.3 (C-2), 144.6 (C-5H), 135.3 (C-1''), 132.2 (C-4''), 131.4 (d, $J = 8.3$ Hz, C-2',6'H), 128.7 (C-3'',5''H), 128.1 (C-7a), 128.1 (C-2'',6''H), 125.8 (d, $J = 3.2$ Hz, C-1'), 119.2 (C-7H), 118.1 (C-6H), 115.8 (d, $J = 22$ Hz, C-3',5'H), 46.9 (benzylic carbon); **¹H-¹⁵N HMBC** (DMSO-*d*₆): [N^1 (147.6 δ ppm): H-6 / H-7 / benzylic CH₂], [N^4 (292.8 δ ppm): H-5 / H-6 / H-7]; **MS** (ESI+) m/z : 338 ($M + H$, 100%), 340 ($M + H + 2$, 32%), 124 ($M + H$, 85%), 126 ($M + H + 2$, 28%), C₁₉H₁₃ClFN₃.

5.1.5.4. 9-(4-Chlorobenzyl)-8-(4-fluorophenyl)-9H-purine (3a), 3-(4-Chlorobenzyl)-8-(4-fluorophenyl)-3H-purine (3b) and 1-(4-Chlorobenzyl)-8-(4-fluorophenyl)-1H-purine (3c). Prepared from **3** (0.15 g) as described in general method. Crude solid (0.166 g) powder was purified by column chromatography. Purification (EtOAc: *n*-Hexane 40: 60) first afforded the compound **3a**, yield 0.004 g, 1.7%. **¹H NMR** δ ppm (CD₃OD): 5.64 (s, 2H, N-CH₂), 7.01–7.04 (m, 2H, H-2'',6''), 7.25–7.32 (m, 4H, H-3',5',3'',5''), 7.73–7.77 (m, 2H, H-2',6'), 8.98 (s, 1H, H-6), 9.13 (s, 1H, H-2); **COSY**: [H-2',6': H-3',5'], [H-2'',6'': H-3'',5'']; **NOESY**: [N-CH₂: H-2',6' / H-2'',6'']; **MS** (ESI+) m/z : 339 ($M + H$, 100%), 341 ($M + H + 2$, 34%), 124 ($M + H$, 91%), 126 ($M + H + 2$, 30%), C₁₈H₁₂ClFN₄.

Continued elution with (EtOAc: *n*-Hexane 55: 45) provided **3b**, as white powder, yield 0.015 g, 6.5%, mp: 165–167°C. **¹H NMR** δ ppm (CDCl₃): 5.77 (s, 2H, N-CH₂), 7.17–7.21 (m, 2H, H-3',5'), 7.37 (d, 2H, $J = 8.4$ Hz, H-3'',5''), 7.46 (d, 2H, $J = 8.4$ Hz, H-2'',6''), 8.42 (s, 1H, H-2), 8.5–8.53 (m, 2H, H-2',6'), 8.9 (s, 1H, H-6); **COSY**: [H-2',6': H-3',5'], [H-2'',6'': H-3'',5'']; **NOESY**: [N-CH₂: H-2 / H-2'',6''];

¹³C NMR, HSQC & HMBC δ ppm (CDCl₃): 170.8 (C-8), 164.8 (d, $J = 250$ Hz, C-4'), 156.2 (C-4), 142.6 (C-5), 142.5 (C-6H), 139.15 (C-2H), 135.6 (C-4''), 131.9 (C-1''), 130.9 (d, $J = 9$ Hz, CH-2',6'), 130.2 (C-2'',6''H), 129.6 (C-3'',5''H), 129.4 (d, $J = 3$ Hz, C-1'), 115.7 (d, $J = 22$ Hz, C-3',5'H), 53.7 (N-CH₂); **¹H-¹⁵N HMBC** (CDCl₃): [N^3 (173.2 δ ppm): H-2 / benzylic CH₂], [N^1 (260.4 δ ppm): H-2 / H-6]; **MS** (ESI+) m/z : 339 ($M + H$, 100%), 341 ($M + H + 2$, 32%), 124 ($M + H$, 95%), 126 ($M + H + 2$, 32%), C₁₈H₁₂ClFN₄.

Continued elution with (CH₂Cl₂: MeOH 100: 4) provided **3c**, yield 0.0735 g, 31%, mp: 269–272°C. **¹H NMR** δ ppm (CD₃OD): 5.67 (s, 2H, N-CH₂), 7.21–7.6 (m, 2H, H-3',5'), 7.44 (s, 4H, H-2'',6'',3'',5''), 8.35–8.37 (m, 2H, H-2',6'), 8.85 (d, 1H, $J = 2$ Hz, H-6), 8.97 (d, 1H, $J = 2$ Hz, H-2); **COSY**: [H-2',6': H-3',5'], [H-2: H-6 (secondary)]; **NOESY**: [N-CH₂: H-2 / H-6 / H-2'',6'']; **¹³C NMR & HSQC & HMBC** δ ppm (CD₃OD): 174.6 (C-8), 167.1 (C-4), 166.2 (d, $J = 248$ Hz, C-4'), 145.8 (C-2H), 138.0 (C-5), 136.45 (C-4''), 135.05 (C-1''), 134.2 (C-6H), 131.8 (d, $J = 9$ Hz, C-2',6'H), 131.1 and 130.6 (C-2'',3'',5'',6''), 130.9 (d, $J = 3.2$ Hz, C-1'), 116.7 (d, $J = 22.5$ Hz, CH-3',5'), 59.9 (N-CH₂); **¹H-¹⁵N HMBC** (CD₃OD): [N^1 (179.3 δ ppm): H-2,6 / benzylic CH₂], [N^3 (259.6 δ ppm): H-2]; **MS** (ESI+) m/z : 339 ($M + H$, 100%), 341 ($M + H + 2$, 30%), 124 ($M + H$, 74%), 126 ($M + H + 2$, 24%), C₁₈H₁₂ClFN₄.

5.2. DFT/B3LYP calculations

The quantum chemical calculations of imidazole-containing heterocycles compounds were performed by choosing DFT, the Becke-3-Lee-Yang-Parr (B3LYP) 6-311 G (d,p) basis set with Gaussian 09 package software [21,22]. Optimization of compounds was done to find the most stable structure with minimal energy and molecular electrostatic potentials (MEP) were calculated. Electronic parameters were measured like HOMO-LUMO energies (ΔE ($E_{\text{LUMO}} - E_{\text{HOMO}}$), ionization potential (IP = $-E_{\text{HOMO}}$), electron affinity (EA = $-E_{\text{LUMO}}$), electronegativity ($X = [IP + EA]/2$), chemical hardness ($\eta = [IP - EA]/2$), chemical softness ($S = 1/2\eta$), chemical potential ($\mu = -[IP + EA]/2$) and electrophilic index ($\omega = \mu^2/2\eta$). The DFT results were evaluated and visualized via the GaussView 6.0 program [23].

5.3. Crystallography

For the crystal structure determination, single-crystal of the compound **2c** and **3c** was used for data collection on a four-circle Rigaku R-Axis RAPID-S diffractometer (equipped with a two-dimensional area IP detector). Graphite-monochromated Mo-K α radiation ($\lambda = 0.71073$ Å) and oscillation scans technique with $\Delta\omega = 5^\circ$ for one image were used for data collection. The lattice parameters were determined by the least-squares methods on the basis of all reflections with $F^2 > 2\sigma(F^2)$. Integration of the intensities, correction for Lorentz and polarization effects and cell refinement were performed using CrystalClear (Rigaku/MSC Inc., 2005) software [24]. The structure was solved by direct methods using SHELXS-97 [25] and non-hydrogen atoms were refined using anisotropic displacement parameters by full-matrix least-squares procedure using the program SHELXL-97 [25]. H atoms were positioned geometrically and refined using a riding model. The final difference Fourier maps showed no peaks of chemical significance. **Crystal data for 2c**: C₁₉H₁₃N₃Cl, crystal system, space group: monoclinic, $P2_1/c$; (no:14); unit cell dimensions: $a = 10.047(3)$, $b = 10.319(3)$, $c = 15.844(5)$ Å, $\alpha = 90$, $\beta = 105.00(8)$, $\gamma = 90^\circ$; volume; 1586.7(8) Å³, $Z = 4$; calculated density: 1.414 g/cm³; absorption coefficient: 0.256 mm⁻¹; $F(000)$: 696; θ -range for data collection 2.1–28.4°; refinement method: full matrix least-square on F^2 ; data/parameters: 3946/218; goodness-of-fit on F^2 : 1.141; final R -indices [$I > 2\sigma(I)$]: $R_1 = 0.055$, $wR_2 = 0.168$, largest diff. peak and hole: 0.533 and -0.525 e Å⁻³. **Crystal data for 3c**: C₁₈H₁₂N₄Cl,

crystal system, space group: triclinic, $P2_1/c$; (no:14); unit cell dimensions: $a = 6.4899(3)$, $b = 18.1279(9)$, $c = 13.4756(7)$ Å, $\alpha = 90$, $\beta = 102.039(1)$, $\gamma = 90^\circ$; volume; $1550.51(9)$ Å³, $Z = 4$; calculated density: 1.451 g/cm³; absorption coefficient: 0.264 mm⁻¹; $F(000)$: 696; θ -range for data collection 2.0 – 28.3° ; refinement method: full matrix least-square on F^2 ; data/parameters: 3848/217; goodness-of-fit on F^2 : 1.090; final R -indices [$I > 2\sigma(I)$]: $R_1 = 0.046$, $wR_2 = 0.143$; largest diff. peak and hole: 0.170 and -0.202 e Å⁻³.

CCDC-2062653 (**2c**) and CCDC-2062824 (**3c**) numbers contain the supplementary crystallographic data for the structures. These data are provided free of charge via the joint CCDC/FIZ Karlsruhe deposition service www.ccdc.cam.ac.uk/structures.

Credit author statement

M.O. Puskullu, F. Doganc, S. Ozden: Synthesis and structure elucidation, E. Sahin: Spectroscopy (XRD crystallography); I. Celik: Calculations (DFT); H. Goker: Synthesis and structure elucidation, Supervision

Declaration of Competing Interest

The authors declare that they have no known competing financial interests or personal relationships that could have appeared to influence the work reported in this paper.

Acknowledgements

Central Laboratory of Pharmacy, Faculty of Ankara University provided support for acquisition of the NMR and mass spectrometer used in this work.

Supplementary materials

Supplementary material associated with this article can be found, in the online version, at [doi:10.1016/j.molstruc.2021.130811](https://doi.org/10.1016/j.molstruc.2021.130811).

References

- [1] M. Krause, H. Foks, K. Gobis, Pharmacological potential and synthetic approaches of imidazo[4,5-*b*]pyridine and imidazo[4,5-*c*]pyridine derivatives, *Molecules* 22 (2017) 399–424, doi:10.3390/molecules22030399.
- [2] F. Doganc, M. Alp, H. Goker, Separation and identification of the mixture of 2-(3,4-dimethoxyphenyl)-1-*n*-propyl or (4-chlorobenzyl)-5 and (6)-1*H*-benzimidazolecarbonitriles, *Magn. Reson. Chem.* 54 (2016) 851–857, doi:10.1002/mrc.4463.
- [3] H. Göker, S. Özden, Regioselective *N*-alkylation of 2-(3,4-dimethoxyphenyl)imidazo[4,5-*b*] and [4,5-*c*]pyridine oxide derivatives: synthesis and structure elucidation by NMR, *J. Mol. Struct.* 1197 (2019) 183–195, doi:10.1016/j.molstruc.2019.07.058.
- [4] C. Karaaslan, F. Doganc, M. Alp, A. Koc, A.Z. Karabay, H. Göker, Regioselective *N*-alkylation of some imidazole-containing heterocycles and their in vitro anticancer evaluation, *J. Mol. Struct.* 1205 (2020) 1–13, doi:10.1016/j.molstruc.2019.127673.
- [5] R. Marek, V. Sklenář, NMR studies of purines, *Annu. Rep. NMR Spectrosc.* 54 (2004) 201–242, doi:10.1016/S0066-4103(04)54005-X.
- [6] P.A. McDonnell, A.D. Gauthier, M.P. Ferro, Differentiation of Regioisomers at ¹⁵N natural abundance using gradient-enhanced ¹H/¹⁵N HMBC NMR spectroscopy, *Magn. Reson. Chem.* 36 (1998) 35–38, doi:10.1002/(SICI)1097-458X(199801)36:1<35::AID-OMR208(3.0.CO;2-A. >
- [7] M. Corredor, J. Bujons, A. Messegue, I. Alfonso, ¹⁵N NMR spectroscopic and theoretical GIAO-DFT studies for the unambiguous characterization of disubstituted 1,2,3-triazoles, *Org. Biomol. Chem.* 11 (2013) 7318–7325, doi:10.1039/C3OB41587B.
- [8] P.M. Chaudhary, S.R. Chavan, M. Kavitha, S.P. Maybhate, S.R. Deshpande, A.P. Likhite, P.R. Rajamohan, Structural elucidation of propargylated products of 3-substituted-1,2,4-triazole-5-thiols by NMR techniques, *Magn. Reson. Chem.* 46 (2008) 1168–1174, doi:10.1002/mrc.2307.
- [9] A. Salgado, C. Varela, A.M.G. Collazo, P. Pevarello, Differentiation between [1,2,4]triazolo[1,5-*a*]pyrimidine and [1,2,4]triazolo[4,3-*a*]pyrimidine regioisomers by ¹H-¹⁵N HMBC experiments, *Magn. Reson. Chem.* 48 (2010) 614–622, doi:10.1002/mrc.2634.
- [10] T.S. Saleh, A.E.M. Mekky, A.S. Al-Bogami, Convergent synthesis strategy of novel fused azines: ¹H-¹⁵N HMBC NMR as a tool for assertion of the site selectivity of Aza-Michael addition reaction, *Curr. Org. Synth.* 13 (2016) 278–290, doi:10.2174/1570179412666150914201114.
- [11] U.D. Phalgune, K. Vanka, P.R. Rajamohan, GIAO/DFT studies on 1,2,4-triazole-5-thiones and their propargyl derivatives, *Magn. Reson. Chem.* 51 (2013) 767–774, doi:10.1002/mrc.4012.
- [12] M.C. Ford, P.S. Ho, Computational tools to model halogen bonds in medicinal chemistry, *J. Med. Chem.* 59 (5) (2016) 1655–1670, doi:10.1021/acs.jmedchem.5b00997.
- [13] C. Bissantz, B. Kuhn, M. Stahl, A medicinal chemist's guide to molecular interactions, *J. Med. Chem.* 53 (14) (2010) 5061–5084, doi:10.1021/jm100112j.
- [14] T.A. Ajayeoba, J.O. Woods, A.O. Ayeni, T.J. Ajayi, R.A. Akeem, E.C. Hosten, O.F. Akinyele, Synthesis, crystallographic, computational and molecular docking studies of new acetophenone-benzoylhydrazones, *J. Mol. Struct.* 1237 (2021) 130275, doi:10.1016/j.molstruc.2021.130275.
- [15] Y.S. Mary, Y.S. Mary, A.S. Rad, R. Yadav, I. Celik, S. Sarala, Theoretical investigation on the reactive and interaction properties of sorafenib-DFT, AIM, spectroscopic and Hirshfeld analysis, docking and dynamics simulation, *J. Mol. Liq.* 330 (2021) 115652, doi:10.1016/j.molliq.2021.115652.
- [16] S. Lahmidi, F. Şen, Y. Sert, F. Uçun, E.M. Essassi, J.T. Mague, A research on structural vibrational, surface characterization of 2-methyl-3-[(5-methyl-[1,2,4]triazolo[1,5-*a*]pyrimidin-7-yl)-4*H*-pyrido[1,2-*a*]pyrimidin-4-one hydrate: SCXRD, FT-IR, MEP, Hirshfeld and Molecular Docking studies, *J. Mol. Struct.* 1235 (2021) 130198, doi:10.1016/j.molstruc.2021.130198.
- [17] D.W. Robertson, E.E. Beedle, J.H. Krushinski, G.D. Pollock, H. Wilson, V.L. Wyss, J.S. Hayes, Structure-activity relationships of arylimidazopyridine cardiotonics: discovery and inotropic activity of 2-[2-methoxy-4-(methylsulfinyl)phenyl]-1*H*-imidazo[4,5-*c*]pyridine, *J. Med. Chem.* 28 (1985) 717–727, doi:10.1021/jm00383a006.
- [18] J. Macdonald, V. Oldfield, V. Bavetsias, J. Blagg, Regioselective C2-arylation of imidazo[4,5-*b*]pyridines, *Org. Biomol. Chem.* 11 (2013) 2335–2347, doi:10.1039/C3OB27477B.
- [19] L. Pan, N. Hang, C. Zhang, Y. Chen, S. Li, Y. Sun, Z. Li, X. Meng, Synthesis and biological evaluation of novel benzimidazole derivatives and analogs targeting the LRP3 inflammasome, *Molecules* 22 (2017) 213–228, doi:10.3390/molecules22020213.
- [20] P.K. Dubey, C.V. Ratnam Formation of heterocyclic rings containing nitrogen: part XXVI-condensation of pyridine 2,3-diamine with aromatic aldehydes, *Proc. Indian Acad. Sci.* 85 (1977) 204–209, doi:10.1007/BF03049482.
- [21] A.D. Beck, Density-functional thermochemistry. III. The role of exact exchange, *J. Chem. Phys.* 98 (7) (1993) 5648–6, doi:10.1063/1.464913.
- [22] C. Lee, W. Yang, R.G. Parr, Development of the Colle-Salvetti correlation-energy formula into a functional of the electron density, *Physical Rev. B* 37 (2) (1988) 785, doi:10.1103/PhysRevB.37.785.
- [23] R. Dennington, T.A. Keith, J.M. Millam, *GaussView V. 6*, SemicheM Inc, Shawnee Mission, KS, 2016.
- [24] Rigaku/MS, Inc., 9009 New Trails Drive, The Woodlands, TX 77381.
- [25] G.M. Sheldrick, A short history of SHELX, *Acta Cryst. A* 64 (2008) 112–122, doi:10.1107/S0108767307043930.